NUMERICAL MODELLING OF THE SEISMIC RESPONSE OF A DEEP EXCAVATION SUPPORTED BY ANCHORED DIAPHRAGM WALLS IN SANDY SOILS

Mario Colil[1], Felipe Villalobos[1] & Rafael Martínez[2]
[1]*Civil engineering department – Universidad Católica de la Santísima Concepción, Concepción, Chile*
[2]*Constructura Lancuyen, Concepción, Chile*

ABSTRACT
The analysis of the seismic response of a deep excavation next to a building and supported by an anchored diaphragm wall in alluvial deposits, is presented. A commercial software using 2D finite element method FEM is used to analyze a stratified profile representative of the Concepcion City Centre, Chile. The 2D FEM is used to study the seismic behaviour by means of the Mohr-Coulomb constitutive model to obtain horizontal displacements and internal forces in the walls, also the vertical displacement of the retained soil is evaluated. The 2010 Chile earthquake acceleration recording on outcropping bedrock in Valparaiso is used as input in the analysis, but scaled to obtain PGA values in free field of 0.21, 0.34 and 0.41g. To calibrate the 2D FEM model, 1D linear-equivalent analyses are compared with 2D FEM analysis in free field conditions (without the excavation) indicating the appropriate horizontal dimension of the 2D FEM model to minimize the reflection effects of the seismic waves. The soil-structure interaction is evaluated by means of acceleration profiles and displacement variations in the wall and retained soil. Finally, estimated anchor force variation versus time in two anchors of different rows is presented.

1. Introduction

Typically, pseudo-static limit equilibrium methods are utilized in the seismic design of retaining structures, the Mononobe-Okabe method is one of the most used (Okabe, 1926; Mononobe, 1929). However, some investigators suggest that this type of simplified method is not appropriate for retaining structures higher than 7 m (O'Riordan and Almufti, 2014). Because of this, the dynamic analysis by means of numerical methods has been developed to investigate the seismic behaviour of deep excavations. However, the realization of this kind of analysis is complex. The response of embedded retaining structures under seismic loading is difficult, because there is a combination of phenomena that make complicated the modelling with sufficient precision. During the propagation of seismic waves in a continuous media in which an excavation has been made, ground amplification occurs which depends on the spatial distribution of rigidities, in the no-linearity of the soil response and on its hysteretic behaviour (Callisto et al., 2008). The difficulty lies in the fact that the numerical modelling must be able to represent the dynamic energy radiation, hysteretic damping of the soil, soil-structure interaction, the propagation of seismic waves and the liquefaction possibility when the ground is saturated (Pathmanathan, 2006).

Special boundary conditions should be used to allow for the radiation of the seismic waves so that they do not rebound back into the model domain accumulating and altering the results. Different boundary conditions have been developed to allow for this radiation (e.g. Kuhlemeyer and Lysmer, 1973). Also, the constitutive model should represent the cyclic behaviour of the soil. Damping is usually considered using the damping coefficient of Rayleigh and Lindsay (1945). Finally, dynamic analyses require special conditions of the maximum size of finite element and horizontal extension of the domain.
The present work aims to contribute to the understanding of the seismic behaviour of deep excavation supported by anchored diaphragm wall using a nonlinear finite element method, especially in the study of the behavior of the anchor lines. Because the propagation of seismic waves strongly depends on the local geology, it has been preferable to develop this work in the alluvial soils of Concepción City Centre in Chile, that are mainly composed of clean sand to silty sands coming from the sediments of the Bío Bío river and also presence of lenses of silt.

2. Methodology

A numerical model has been used which corresponds to the 2D finite element method of the commercial software Plaxis 2D V 8.2 (2009) for the seismic analysis of an anchored diaphragm wall supporting a 14 m deep excavation and next to a 4 storey building. A surcharge of 50 kPa located 1 m behind the diaphragm wall, with an extension of 16 m simulates the presence of the building. The ground stratigraphy was obtained from a deep borehole carried out in Concepcion City Centre, Chile (Dobry and Poblete, 1968; Poblete 1967). Prior to the seismic analyses, the construction sequence steps were

simulated. These sequences and the computational steps modeled in this work are detailed below.

Stage 1: initial stress state (K_0 method)
Stage 2: activation of the surcharge
Stage 3: activation of the diaphragm wall (wished-in-place)
Stage 4: excavation stage 1 (to level -3.5 m)
Stage 5: activation of anchor 1 at level -3.0 m with an inclination of 20° with respect to the horizontal
Stage 6: water lowering to -10 m
Stage 7: excavation stage 2 (to level -9.0 m)
Stage 8: activation of anchor 2 at level -8.5 m with an inclination of 20° with respect to the horizontal
Stage 9: water lowering to -15 m
Stage 10: excavation stage 3 (to level -14 m)
Stage 11: reset displacement to zero and application of the seismic load

The transversal component of the 27F earthquake of 2010 measured in outcropping bedrock at the UTFSM with PGA of 0.30 g as input in the base of the numerical model, was used. This recording was scaled to obtain in surface PGA values of 0.21, 0.34 and 0.41g in free field conditions.

The alluvial soil deposits under study corresponds to silty sand with the incorporation of four silt lenses located at 24.9, 34.4, 56.6 and 75.1 m depth. The friction angles of the granular soils were obtained from correlations between ϕ and $(N_1)_{60}$ by the expression of Peck et al. (1974). The undrained shear strength of the silt lenses were obtained from unconfined compression tests (Poblete, 1967). Figure 1 shows the shear wave velocity and the maximum shear modulus variation with depth of the soil deposits obtained from downhole tests and laboratory tests (Poblete, 1967).

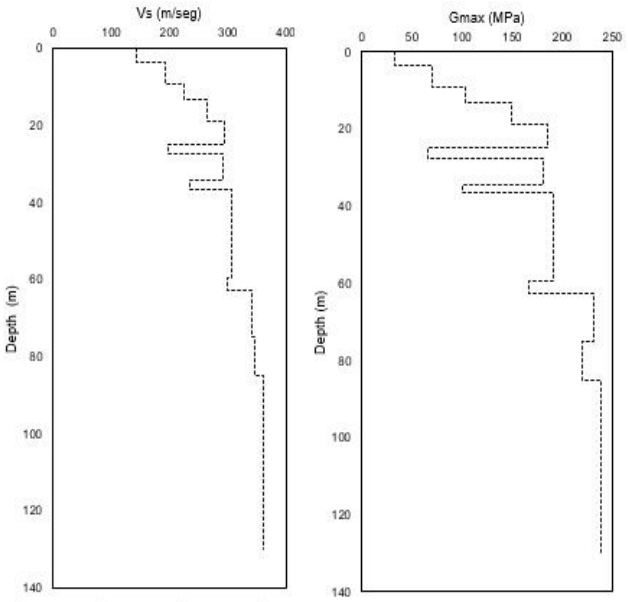

Fig 1. Shear wave velocity profile obtained from a deep borehole in Concepcion City Centre, Chile (Poblete, 1967).

The degradation curves for sand of Seed and Idriss (1991) and the degradation curves for cohesive soils of Vucetic and Dobry (1991) were used to consider the reduction of the shear modulus and the damping level with shear deformation by iterating up to converge to a fixed ratio.

It has been assumed that a granite rock begins at a depth of -130 m and correspond to the bedrock of the deposit (Poblete, 1967). The phreatic level has been located at -6.5 m depth according to drilling data.

Soil damping was calculated from the coefficient of Rayleigh and Lindsay (1945) α and β, using equation [1]:

$$\begin{bmatrix}\alpha\\ \beta\end{bmatrix} = \frac{d}{\pi(f_i + f_j)}\begin{bmatrix}4\pi^3 f_i f_j\\ 1\end{bmatrix} \qquad [1]$$

Where d is the damping ratio and f_i and f_j are vibrating frequencies of the i and j mode of the system. To obtain the Rayleigh coefficients, the frequencies associated to the first two vibration modes of the soil deposits were used, the values of these frequencies are f_1 = 0.57 Hz y f_2 = 1.72 Hz.

Typically, the damping levels used to model the soil are in the range of 2 to 5%. Since there were no dynamic tests such as resonance column tests, a constant value of d = 3% was used for silty sand and d = 4% was used for silts, values corresponding to a shear deformation level of 0.018 and 0.016 % respectively, and Rayleigh coefficients were calculated for each of them.

Table 1 presents the geomechanical and dynamic properties of the soil deposit to be modeled, the profile consist of 13 soil layers.

The seismic response is studied considering that the soil has an elastoplastic behaviour using the Mohr-Coulomb constitutive model. The analyses were carried out under undrained conditions due to the rapid loading implied by an earthquake. Due to the limitations of the model, the evaluation of the liquefaction potential was not part of the study, besides the high Nspt values would indicate that there is no liquefaction potential in the sandy strata.

A linear elastic model with Poisson's ratio of 0.20 and a Young modulus of 24870 MPa was used for the reinforced concrete diaphragm wall of 0.80 m of thickness and 20 m of length. In the simulation, the installation of the diaphragm wall is modelled as wished-in-place (WIP), which does not consider the effect of the installation on soil movements and the behaviour in subsequent excavation stages. Interface elements with a reduction strength factor R_{int} = 0.80 were considered between concrete and granular soil.

The anchor lines with cement grout were modeled using node-to-node anchoring elements for the free length, the bulb were modeled using a membrane element that transmit axial forces but not flexure. This element in Plaxis is denoted by a geogrid element which guarantees the transfer of load to the ground along the bonded length and avoids the concentration of point load at the end of the free length.

Table 1. Geomechanical and dynamic properties of the soil deposit to be modeled.

Layers	H1	H2	H3	H4	H5	H6	H7	H8	H9	H10	H11	H12	H13
USCS	SM	SM	SM	SM	SM	MH	SM	ML	SM	ML	SM	MH	SM
Depth (m)	3.5	9.4	13.4	19.0	24.9	27.5	34.4	36.5	59.6	62.8	75.1	85.0	130.0
Thickness (m)	3.5	5.9	4.0	5.6	5.9	2.6	6.9	2.1	23.1	3.2	12.3	9.9	45.0
γ (kN/m^3)	16.0	19.00	20.0	21.0	21.0	17.0	21.0	18.0	20.0	18.0	20.0	18.0	18.0
E_0 (MPa)	85.0	184.0	267.0	388.0	481.0	179.0	472.0	269.0	495.0	448.0	602.0	595.0	618.0
G_0 (MPa)	33.0	71.0	103.0	149.0	185.0	66.0	182.0	100.0	190.0	166.0	232.0	221.0	238.0
ϕ (°)	34.0	36.0	40.0	42.0	42.0	---	42.0	---	42.0	---	42.0	---	42.0
ψ (°)	4.0	6.0	10.0	12.0	8.0	---	6.0	---	0.0	---	0.0	---	0.0
S_u (kPa)	---	---	---	---	---	66.0	---	66.0	---	92.0	---	150.0	---
d (%)	3.0	3.0	3.0	3.0	3.0	4.0	3.0	4.0	3.0	4.0	3.0	4.0	3.0

A horizontal separation between anchor lines of 1.0 m and a axial stiffness of AE = 200 MN/m were considered, while the axial stiffness used in the bulbs corresponds to AE = 100 MN/m.

In this modelling, it has been decided to use the triangular element of 15 nodes because it delivers more precise results by having more number of nodes, however, a disadvantage is the high memory consumption and a relatively slow calculation.

With regard to boundary conditions for dynamic time domain analysis using the 2D FEM, the viscous boundary of Kuhlemeyer and Lysmer (1973) was used at the lateral edges, while the base of the model was considered rigid, the use of a rigid boundary at the base is reasonable considering the high impedance contrast of the granitic rock that underlies the model base.

Dynamic numerical analysis requires an appropriate dimension of finite elements to avoid the numerical distortion of wave propagation in the soil. Kuhlemeyer and Lysmer (1973) recommend that the lengths of the elements ΔL should be less than one tenth to one eighth of the wavelength λ associated with the highest frequency of the earthquake. The size of the finite element mesh can then be selected according to equation [2].

$$\Delta L = \frac{V_s}{A f_{max}} \qquad [2]$$

Where A can take different values according to the software recommendations, *A = 8* was used in this analysis.

To calibrate the 2D FEM model, the results were compared with 1D analysis using the equivalent linear method with the Deepsoil V 6.1 software (Hashash, 2015).

3. Characteristics of the earthquake

An acceleration record measured on outcropping rock was used for the dynamic analysis, this corresponds to the transverse component of the February 27 earthquake of moment magnitude Mw = 8.8 measured at the UTFSM station in Valparaíso, Chile on volcanic rock. In Concepcion, this earthquake was measured at the station located in Colegio Inmaculada Conception, where the soil corresponds to deposits of saturated sand, the PGA value measured at this station was 0.40g for the longitudinal component and 0.29g for the transverse direction. Figure 2 shows the acceleration record measured in Valparaíso on outcropping rock, the record has a duration of 72 s and a PGA of 0.30 g, the sampling frequency was 200 Hz.

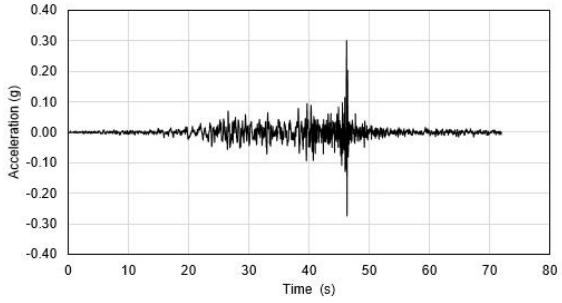

Fig 2. Acceleration record, transversal component measured at the UTFSM station in Valparaíso (RENADIC 2010).

4. Free field response

The effect of the horizontal distance of the vertical edges of the model is relevant in dynamic analyses, regarding this, Amorosi et al. (2010) indicate that with a horizontal dimension of B = 6H there would be good results, where H is the vertical dimension of the model and B the horizontal dimension. Visone (2008) used a horizontal dimension of B = 30H to model the seismic response of an embedded retaining structure.

The responses for B = 2H; 6H and 30H were compared, and it was observed that as the horizontal dimension of the model increases, the response in terms of acceleration profile and shear stresses approaches the results obtained from the 1D analysis.

The domain of the model used has a vertical dimension H = 130 m and horizontal B = 30H = 3900 m. The size of the finite elements was adjusted in Plaxis by means of the average element size AES and this was left in ΔL =1.78 to 4.0 m. The model has 19020 finite elements, 153801 nodes and 228240 stress points. The model has been divided into three zones with a width of B/3 each, in the central zone the finite element mesh has been refined, while in the lateral zones it has been refined to a lesser extent to improve the dissipation of the seismic waves which are directed towards the lateral boundaries of the model.

Figure 3 shows half of the domain analyzed together with the finite element mesh, the mesh density progressively decreases as it approaches the vertical edge of the model, allowing a better dissipation of seismic waves, equation [2] is only valid for the central part of the model.

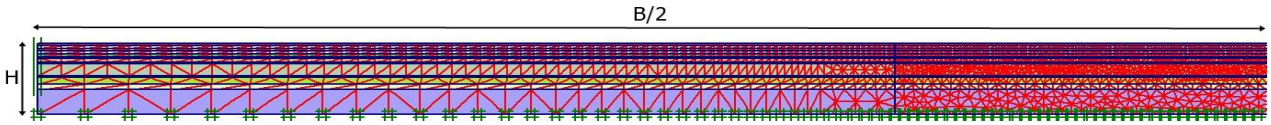

Fig 3. Left half of the dynamic finite element mesh of the model.

With regard to the configuration used in Plaxis to perform the dynamic analysis using the Mohr-Coulomb constitutive model, the number of "Additional steps" was left as 1000, on the other hand the time step for the dynamic analysis is calculated by equation 3.

$$\delta t = \frac{\Delta t}{mn} \qquad [3]$$

Where δt is the time step, Δt is the duration of the seismic record, *m* is the number of additional steps and *n* is the number of dynamic sub-steps. The value of the multiplication *mn* gives the total number of steps to be used in the discretization of the time, being important to establish an adequate number of steps so that the input of the seismic record is correctly covered in the analysis. When using δt = 0.005 s corresponding to the sampling frequency of the seismic record (200 Hz), *m* = 1000 which is the maximum number of additional steps and Δt = 72 s for the earthquake, so the number of sub-steps is *n* = 14.

The following is a comparison of the artificial records obtained on the surface from the 1D analysis using the linear equivalent method and the 2D modeling using the Mohr-Coulomb constitutive model. The PGA for the 1D model is 0.34g, while the 2D model for B = 2H is 0.36g, for B = 6H and B = 30H is 0.34 g. It is clear that the increase in the horizontal dimension of the model allows the dissipation of the seismic waves preventing the reflection effects of accumulating energy within the numerical model. Figure 4 shows that the 1D and 2D models provide similar acceleration pulses, in general, the accelerations are greater in the 2D model.

The obtained results indicate that the distributions of maximum accelerations and of shear deformations have relatively similar magnitudes, giving the 1D (EQL) and 2D models almost identical surface PGA values

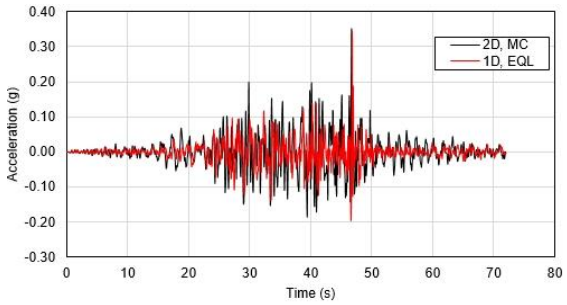

Fig 4. Comparison of surface acceleration records using 1D and 2D modeling.

The 1D analysis using the equivalent linear method gives a fundamental surface period of 0.32 s, while the 2D model has a period of 0.33 s and the surface PGA for both models is 0.34 g, so the calibration assumed is satisfactory for B = 30H.

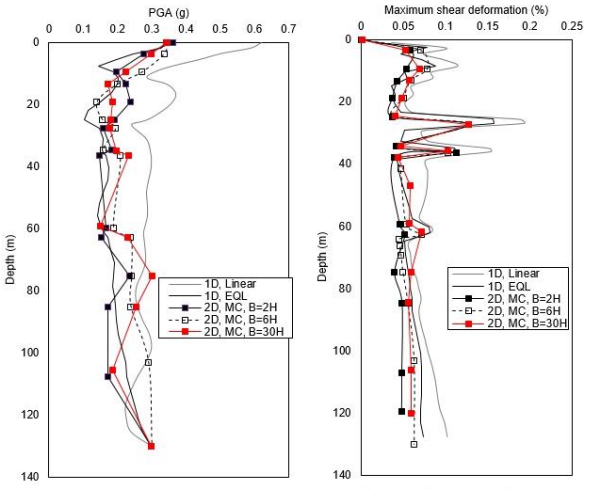

Fig 5. Comparison of the acceleration and maximum shear deformations profiles obtained by the 1D and 2D analyzes.

To reduce the computational cost, the response for B = 6H is also considered satisfactory, which is also proposed by Amorosi et al. (2010).

Because the PGA value measured at the Colegio Inmaculada Conception Station was 0.40 g, the transversal component of the seismic record measured in Valparaiso was scaled to obtain a surface PGA value of 0.20g and 0.40g in order to study the seismic behaviour for different PGA values. The acceleration record was scaled at 0.45 g and 0.18 g to obtain on the surface values of 0.41 g and 0.21 g respectively. These accelerations records will be used for seismic analysis of the excavation supported by an anchored diaphragm wall.

5. Seismic response of excavation

Figure 6 shows the domain of the finite element model used to consider soil-structure interaction under seismic loading. Since in the calibration stage the dynamic response of the model for a dimension of B = 6H is similar to that obtained for the condition of B = 30H, the soil-structure interaction models with B = 6H were used. The domain consists of the central part of the model with horizontal dimension Bc = 2H with a fine density mesh with a 2.0 m finite element average dimension and two lateral domains with horizontal extension BL = 2H with a thick mesh of finite elements to aid in the dissipation of seismic waves (Visone, 2008).

Rayleigh coefficients are added to the properties of the diaphragm wall to consider the damping of this material, $\alpha = \beta = 0.001$ has been used (Ibrahim and Ibrahim, 2013).

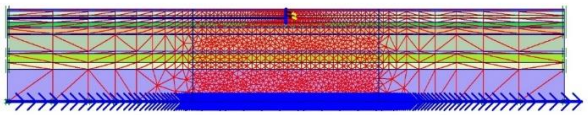

Fig 6. Finite element mesh used in dynamic analysis considering soil-structure interaction.

The PGA profiles for the three seismic registers scaled at 0.18, 0.30 and 0.45g used in the base of the model and their evolution in the first 20 m depth of the numerical model are shown in Figure 7 showing the effect of a 14 m depth excavation. In free field conditions (without excavation) the maximum accelerations obtained at the surface are 0.21, 0.34 and 0.41g respectively, while due to the excavation the maximum accelerations obtained (just behind the excavation) are 0.25, 0.38 and 0.47g indicating the increase in the seismic demand product of the excavation. In addition, the maximum surface accelerations under free field condition and the acceleration used in the pseudostatic design Ar = 0.24g (NCh 3206, 2010) are shown. The amplification of the accelerations is due to the change of geometry, which disturbs the arrival of the shear waves and the loss of rigidity due to the excavation.

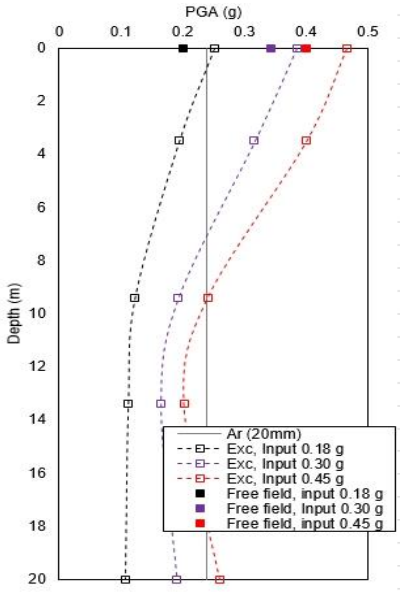

Fig 7. Evolution of PGA with depth due to excavation.

6. Displacements

The evaluated system considers a surcharge of 50 kPa distributed in a length of 16 m. This surcharge is located 1 m behind the diaphragm wall of 20 m length, and simulates the presence of a building of 4 stories in height.

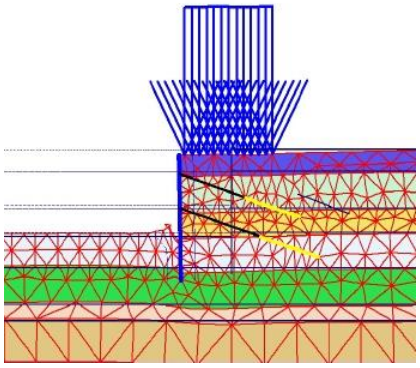

Fig 8. Deformed mesh for PGA =0.38 g in surface.

Figure 9 shows the estimated maximum horizontal displacement of the anchored diaphragm wall for the seismic record imposed at the base of the model. It is observed that this depends strongly on the duration of the input ground motion and the number of pulses of the acceleration record. At the beginning, the horizontal displacements increase steadily until around 22 s and then stronger oscillatory wall movements can be observed due to the changes in the acceleration record. The maximum displacements reached correspond to Ux =10.2, 19.3 and 34.2 cm for PGA values of 0.25, 0.38 and

0.47 g respectively, while the final displacements at the end of the earthquake are Ux = 9.56, 18.1 and 32.4 cm showing the possible significant effect of permanent seismic induced horizontal displacements.

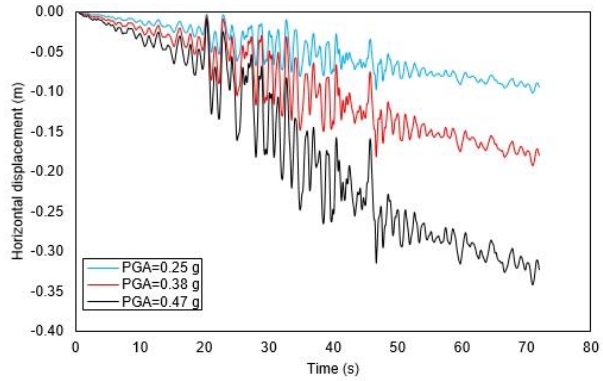

Fig 9. Comparison of records of horizontal displacements with respect to time.

Figure 10 shows the comparison of the vertical displacements estimated immediately behind the wall, where the largest settlement of the soil surface occurs. The maximum settlements reached correspond to Uy = 1.3, 2.3 and 2.7 cm for PGA values of 0.25, 0.38 and 0.47 g respectively, while the displacements in the final stage of the earthquake are Uy = 1.1, 1.9 and 2.2 cm. When using the Mohr-Coulomb model these values of settlements may be unrealistic showing a recovery between 2 to 5 mm for the cases analyzed due to the inability of the constitutive model to distinguish between loading and unloading trajectories, however, these results can be used as a first approximation to the magnitude of the expected settlements.

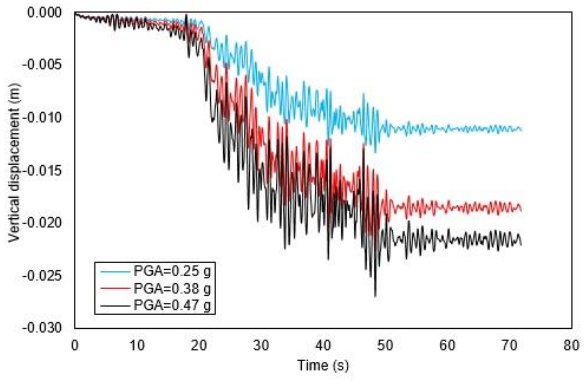

Fig 10. Comparison of vertical displacements with time, 1 m behind the wall for three input acceleration records.

7. Internal forces

Figure 11 shows the diagrams of bending moments and shear forces for a PGA of 0.25 g obtain by Plaxis. In addition, they are compared with the results obtained with GGU-Retain (2008) software using the pseudostatic method with a pseudo-acceleration of Kh=0.24 g. It is observed that in general the results obtained under limit equilibrium are similar to those obtained by numerical modelling, being the last one more conservative resulting in greater bending moments. The maximum moments and shear forces obtained by the pseudostatic method are slightly higher than those obtained numerically.

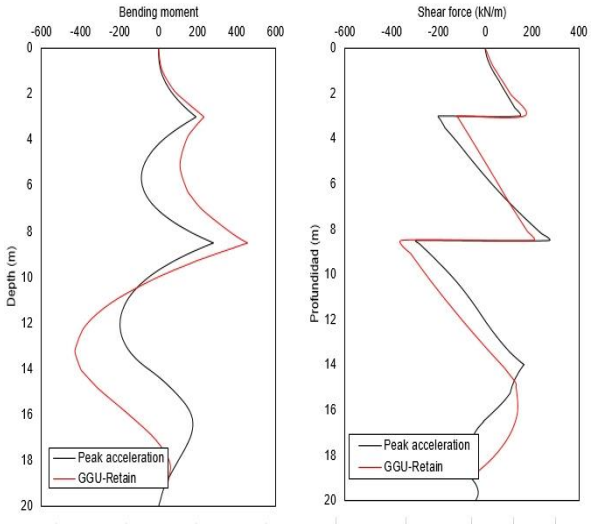

Fig 11. Distribution with depth of bending moments and shear forces at the end of the earthquake.

Table 2 shows the maximum bending moments generated on the diaphragm wall for the three scaled seismic records used in the analysis. The time at which the maximum acceleration occurs, is related to the maximum horizontal displacement of the diaphragm wall.

Table 2 Bending moments generated on the diaphragm wall (kNm/m).

PGA (g)	GGU-Retain	End of earthquake	At max. acceleration	Maximum
0.25	427	292.7	279.8	313.9
0.38	427	320.5	295.2	345.6
0.47	427	331.4	300.3	363.7

8. Anchor lines

The study of numerical time-history simulations allows to obtain the variation of the load in an anchor during a seismic event. These variations are shown for the upper and lower anchor lines for the scaled seismic record that causes 0.41g in surface in free field condition and 0.47g due to the excavation in Figures 12 and 13 respectively.

Moreover, the comparison is made with results from the last static step of the numerical simulation with Plaxis. The load on the anchors has been discretized every 2 s which leads to a loss of information, however, care has been taken to obtain the maximum load of the anchor measured in the peak time of accelerations.

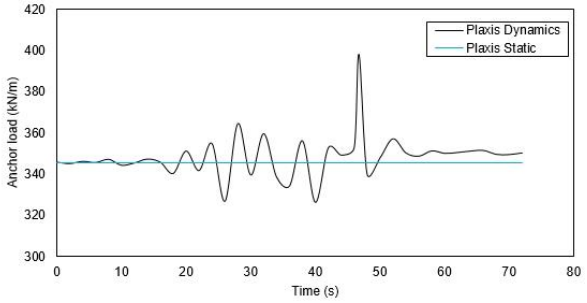

Fig 12. Evolution of the load at the upper anchor, PGA = 0.47g.

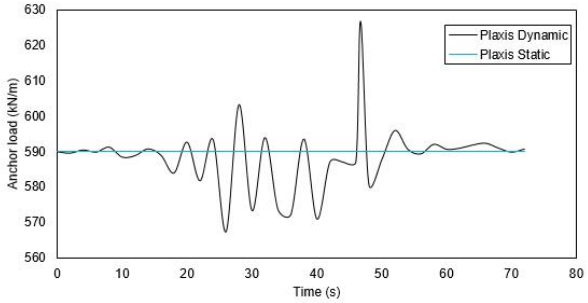

Fig 13. Evolution of the load at the lower anchor, PGA= 0.47g.

Tables 3 and 4 show the loads in the upper and lower anchor lines obtained in the final construction stage, the maximum load experienced by the anchor lines during the time-history numerical modelling, the load at the end of the earthquake and the seismic increment in load anchor Δ between the maximum dynamic load and the static load. For a surface, PGA of 0.25g the maximum load obtained for the upper anchor line during the seismic modelling is 6.4% greater than that obtained in the last static stage, whereas for the lower anchor line it is 2.2% greater.

Table 3. Load in upper anchor line (kN /m), dynamic analysis.

PGA (g)	Final static stage	Maximum	End of earthquake	Δ % Increment
0.25	345.7	368.3	343.7	6.4
0.38	345.7	384.7	348.8	11.3
0.47	345.7	398.2	350	15.0

Table 4. Load in lower anchor line (kN /m), dynamic analysis.

PGA (g)	Final static stage	Maximum	End of earthquake	Δ % Increment
0.25	590	603.3	586.1	2.2
0.38	590	616.0	588.1	4.4
0.47	590	626.8	590.8	6.3

9. Conclusions

A numerical analysis was carried out using the 2D nonlinear finite element method of the seismic response of an anchored diaphragm wall in alluvial soil and water table representing the geological and geotechnical context of the center of Concepción, Chile.

The horizontal dimension of the 2D model was calibrated from the results of propagation of shear waves in 1D in free field. The results indicated that there is a strong relationship between the horizontal dimension of the model and the profile of accelerations and shear deformations. It was determined that for B = 6H the profile of horizontal maximum accelerations and shear deformations was similar to that obtained in 1D modelling as previously observed by Amorosi et al. (2010). The results also indicated that the surface PGA obtained by the 2D model is 0.34g while using the equivalent linear method in 1D is 0.35g which indicates that for B = 6H a better radiation damping is achieved

The maximum moments and shear forces obtained by the pseudostatic method are slightly higher than those obtained numerically. These results would indicate that the limit equilibrium method covers well the internal stresses to which an anchored retaining structure is being subjected, at least this is observed in this investigation.

In general, the load obtained in the last static stage (excavation up to 14 m depth) is similar to that obtained in the time-history analysis for the end of the earthquake, however, the load experienced at the moment of the peak acceleration of the seismic register is slightly higher. In the order of 6.4 to 15 % for the upper anchor and 2.2 to 6.3 for the lower anchor.

The major increment in the upper anchor may be due the inclination of the anchor and the differential movement between the upper part of the diaphragm wall and the end of the free length of the anchor.

10. References

Amorosi, A., Boldini, D., and Elia, G. 2010. *Parametric study on seismic ground response by finite element modelling*. Computers and Geotechnics 37(4), 515-528.

Boroschek, R., Soto, P., and Leon, R., (2010). *Maule region earthquake, February 27, 2010, Mw = 8.8. RENADIC Report 10/08*. Published electronically at http://www.cec.uchile.cl/ renadic/red.html. (Last access 13/09/2010). (In Spanish).

Callisto, L., Soccodato, F., and Conti, R. 2008. *Analysis of the Seismic Behaviour of Propped Retaining Structures*. Geotechnical Earthquake Engineering and Soil Dynamics IV, 1-10.

Dobry, R. and Poblete, M. (1968). *Modelo dinámico del subsuelo de Concepción*. Revista del IDIEM 7(3), 111-136.

GGU-RETAIN. 2008. Analysis and design of sheet pile walls, soldier pile walls and in-situ concrete walls to EAB. GGU Zentrale Verwaltung mbH, Braunschweig.

Hashash, Y. 2015. Deepsoil. Urbana-Champaign: Tutorial and User Manual. University of Illinois, 2.

Ibrahim, K. M. H. I., and Ibrahim, T. E. 2013. Effect of historical earthquakes on pre-stressed anchor tie back diaphragm wall and on near-by building. HBRC Journal, 9(1), 60-67.

Kuhlemeyer, R. L., and J. Lysmer. 1973. *Finite Element Method Accuracy for Wave Propagation Problems*. J. Soil Mech. & Foundations, Div. ASCE, 99(SM5), 421-427.

Mononobe, N., and Matsuo, H. 1929. *On the determination of earth pressure during earth-quakes*. In Proceedings of the World Engineering Conference, (9):179- 187.

NCh 3206. 2010. Geotécnia - Excavaciones, entibaciones y socalzados. NN, Santiago, Chile.

O'Riordan N. and Almufti, I. 2014. *Seismic stability of braced excavations next to tall buildings*. Proceedings of the ICE Geotechnical Engineering 168(1): 31-41.

Okabe, S. 1924. General theory of earth pressure and seismic stability of retaining wall and dam. J.Japan Soc. Civ Engrs, Tokyo, Japan, 12(1).

Pathmanathan, R. 2006. *Numerical modelling of seismic behaviour of earth-retaining walls*. M.Sc. thesis, Rose School, Pavia, Italy.

Peck, R. B., Hansen, W. E., and Thornburn, T. H. 1974. Foundation Engineering. Wiley & Sons, New York, NY, USA.

Plaxis 2D. 2009. *Plaxis bv, Delft*, the Netherland.

Poblete, M. (1967). El suelo del centro de Concepción en relación con el diseño antisísmico. Thesis, University of Chile, Santiago, Chile.

Rayleigh, J. W. S. and Lindsay, R. B. 1945. *The Theory of Sound*. Dover Publications, New York, NY, USA.

Seed H.V., and Idriss I.M. 1970. *Soil moduli and damping factors for dynamic response analysis*., Technical report EERRC-70-10, University of California, Berkeley, CA, USA.

Visone, C. 2008. *Performance-Based approach in seismic design of embedded retaining walls*. PhD, thesis, Università degli Studi di Napoli Federico II, Italy.